Discovery of Hard Nonthermal Pulsed X-Ray Emission from the Anomalous X-Ray Pulsar 1E 1841-045

Kuiper, L.; Hermsen, W.; Mendez, R.M.

Published in:
Astrophysical Journal

DOI:
10.1086/423129

The Astrophysical Journal, 613:1173–1178, 2004 October 1

DISCOVERY OF HARD NONTHERMAL PULSED X-RAY EMISSION FROM THE ANOMALOUS X-RAY PULSAR 1E 1841−045

L. Kuiper,[1] W. Hermsen,[1,2] and M. Mendez[1,2]
Received 2004 April 29; accepted 2004 June 4

ABSTRACT

We report the discovery of nonthermal pulsed X-ray/soft gamma-ray emission up to ∼150 keV from the anomalous 11.8 s X-ray pulsar AXP 1E 1841−045 located near the center of supernova remnant Kes 73 using *Rossi X-Ray Timing Explorer* (*RXTE*) Proportional Counter Array and High Energy X-Ray Timing Experiment (HEXTE) data. The morphology of the double-peaked pulse profile changes rapidly with energy from 2 keV up to ∼8 keV, above which the pulse shape remains more or less stable. The pulsed spectrum is very hard; its shape above 10 keV can be described well by a power law with a photon index of 0.94 ± 0.16. 1E 1841−045 is the first AXP for which such very hard pulsed emission has been detected, which points to an origin in the magnetosphere of a magnetar. We have also derived the total emission spectrum from the Kes 73/1E 1841−045 complex for the ∼1–270 keV energy range using *RXTE* HEXTE and *XMM-Newton* pn data. A comparison of the total emission from the complex with the pulsed+DC emission from 1E 1841−045 as derived from *Chandra* ACIS CC-mode data (Morii et al. 2003) leaves little room for emission from Kes 73 at energies near 7 keV or above. This suggests that the HEXTE spectrum above ∼15 keV, satisfactorily described by a power law with index 1.47 ± 0.05, is dominated by emission from 1E 1841−045. In that case the pulsed fraction for energies above 10 keV would increase from about 25% near 10 keV to 100% near 100 keV. The origin of the DC-component extending up to ∼100 keV is probably magnetospheric and could be a manifestation of pulsed emission that is "on" for all phases.

Subject headings: pulsars: individual (1E 1841−045) — X-rays: stars

1. INTRODUCTION

The question of whether anomalous X-ray pulsars (AXPs) and soft gamma-ray repeaters (SGRs) are both manifestations of isolated neutron stars with ultrastrong magnetic fields ($\sim 10^{14}$–10^{15} G), so-called magnetars (Thompson & Duncan 1996), has recently been decided. Notably, the first detection of SGR-like bursts from the direction of AXP 1E 1048.1−5937 (Gavriil et al. 2002), followed by the detection of SGR-like bursts from AXP 1E 2259+586 (Kaspi et al. 2003) conclusively unified AXPs and SGRs (see also Gavriil et al. 2004). Similarly, Kulkarni et al. (2003) showed that the originally classical SGR 0526−66 was recently found to behave like an AXP. This was predicted uniquely by the magnetar model (Thompson & Duncan 1996). For recent reviews on AXPs and SGRs, see Mereghetti et al. (2002) and Woods (2004).

In this paper we present detailed timing and spectral characteristics of AXP 1E 1841−045, located in the center of the supernova remnant (SNR) Kes 73 (G27.4+0.0), which is at a kinematic distance between 6 and 7.5 kpc (Sanbonmatsu & Helfand 1992). The 11.8 s X-ray pulsations of the source were discovered with *ASCA* (Vasisht & Gotthelf 1997), and a phase-connected timing solution was published by Gotthelf et al. (2002), who analyzed observations with the *Rossi X-Ray Timing Explorer* (*RXTE*) spanning 2 years. A linear ephemeris appeared to be consistent with the pulse periods measured over 15 years with *Ginga*, *ASCA*, *RXTE*, and *BeppoSAX*. The measured constant, long-term spin-down of 1E 1841−045, as well as the phase-connected timing with "timing-noise–like" residuals, supported a magnetar identification.

Morii et al. (2003) reported detailed results for 1E 1841−045 from *Chandra* ACIS CC-mode observations. They could for the first time discriminate the compact object from the surrounding SNR Kes 73. Like other AXPs, the phase-integrated spectrum (pulsed and DC emission) was well fitted with a power law (photon index 2.0 ± 0.3) plus blackbody model ($kT_{\rm BB} = 0.44 \pm 0.02$ keV). The photon index is the flattest among AXPs. It should be noted, however, that a two-blackbody fit rendered a similarly good fit. They also reported that the pulse profile is double-peaked, with the second pulse exhibiting a harder spectrum between 3 and 7 keV.

Molkov et al. (2004) recently published a source catalog of 28 sources detected by the *INTEGRAL* IBIS between 18 and 120 keV in a survey of the Sagittarius Arm tangent region. The source in this catalog with the hardest spectrum was identified with 1E 1841−045 and SNR Kes 73. Since AXPs are "known" to be soft-spectrum sources, the SNR seemed at first glance the most likely counterpart. This identification stimulated us to analyse archival *RXTE* Proportional Counter Array (PCA) and High Energy X-Ray Timing Experiment (HEXTE) data to search for a pulsed signature from 1E 1841−045, particularly in the hard X-ray range covered by HEXTE. We also analyzed archival *XMM-Newton* data in an attempt to unravel the contributions from Kes 73 and the pulsed and unpulsed emissions from 1E 1841−045, combining the information from our *RXTE* PCA/HEXTE and *XMM-Newton* analyses and the *Chandra* results on 1E 1841−045 published by Morii et al. (2003).

2. INSTRUMENTS AND OBSERVATIONS

In this study the results come mainly from the analysis of data from two of the three X-ray instruments on board *RXTE*, the PCA (2–60 keV) and HEXTE (15–250 keV). Both are nonimaging instruments. The PCA (Jahoda et al. 1996) consists

[1] SRON-National Institute for Space Research, Sorbonnelaan 2, 3584 CA, Utrecht, Netherlands; l.m.kuiper@sron.nl.
[2] Astronomical Institute "Anton Pannekoek," University of Amsterdam, Kruislaan 403, 1098 SJ Amsterdam, Netherlands.

TABLE 1
List of RXTE Observations Used in this Study of 1E 1841−045

Observation ID	Begin Date	End Date	Exposure Time[a] (ks)
40083.....	1999 Feb 15	2000 Feb 23	105.73
50082.....	2000 Apr 10	2001 Mar 8	59.91
60069.....	2001 Apr 2	2002 Jan 26	52.24
70094.....	2002 Mar 16	2003 Jan 27	53.26

[a] PCU-2 exposure after screening.

of five collimated xenon proportional counter units (PCUs) with a total effective area of $\sim$6500 cm^2 over a $\sim 1^\circ$ (FWHM) field of view. Each PCU has a front propane anticoincidence layer and three xenon layers, which provide the basic scientific data, and is sensitive to photons with energies in the range 2–60 keV. The energy resolution is about 18% at 6 keV.

The HEXTE instrument (Rothschild et al. 1998) consists of two independent detector clusters, each containing four NaI(T1)/CsI(Na) scintillation detectors. The HEXTE detectors are mechanically collimated to a $\sim 1^\circ$ (FWHM) field of view and cover the 15–250 keV energy range with an energy resolution of $\sim$15% at 60 keV. The collecting area is 1400 cm^2, taking into account the loss of the spectral capabilities of one of the detectors. The maximum time resolution of the tagged events is 7.6 μs. In its default operation mode the field of view of each cluster is switched on and off source to provide instantaneous background measurements. Because of the coalignment of HEXTE and the PCA, they simultaneously observe the sources in their field of view. Table 1 lists the publicly available *RXTE* observations used in this study.[3] All observations listed in Table 1 have been carried out with the instrumental pointing axis within $\sim 0.'5$ from 1E 1841−045. In the fourth column the PCU unit 2 screened exposure is given (see § 3.1). A typical observation run consists of several subobservations spaced more or less uniformly between the start and end date of the observation. In this study the total number of subobservations amounts 45.

3. TIMING ANALYSIS

3.1. *Timing Analysis of PCA Data*

The PCA data from the observations listed in Table 1 have all been collected in *Goodxenon* or *GoodxenonwithPropane* mode allowing high time resolution (0.9 μs) studies in 256 spectral channels. Because we are mainly interested in the medium/hard X-ray timing properties of 1E 1841−045, we ignored the events triggered in the propane layers of each PCU. Furthermore, we used only data from the top xenon layers of each PCU in order to improve the signal-to-noise ratio. Because the number of active PCUs at any time was changing, we treated the five PCUs constituting the PCA separately. For each PCU good time intervals have been determined by including only time periods when the PCU in question is on and during which the pointing direction is within $0.^\circ 05$ from the target, the elevation angle above Earth's horizon is greater than 5°, a time delay of 30 minutes since the peak of a South Atlantic Anomaly passage holds, and a low background level from contaminating electrons is observed. These good time intervals have subsequently been applied in the screening process to the data streams from each of the PCUs (e.g., see Table 1 for the resulting screened exposure of PCU-2 per observation run).

[3] 1E 1841−045 has been regularly monitored by *RXTE* since 1999 February.

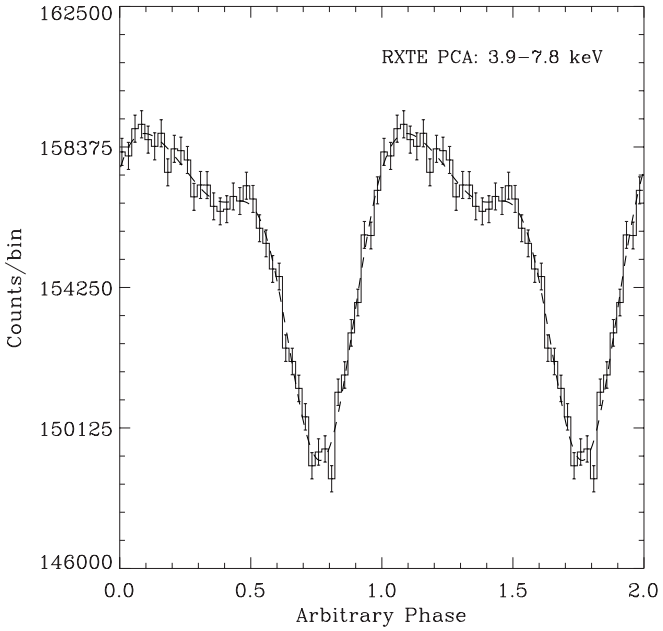

Fig. 1.—*RXTE* PCA pulse profile of 1E 1841−045 for energies in the range 3.9–7.8 keV combining data collected between 1999 February and 2003 February (see Table 1). Two cycles are shown for clarity. The best-fitting truncated Fourier series (three harmonics) is superposed as a dashed line.

Next, for each subobservation the arrival times of the selected events (for each PCU unit) have been converted to arrival times at the solar system barycenter (in TDB timescale) using the instantaneous spacecraft position and celestial position of 1E 1841−045 (see Gotthelf et al. 2002). These barycentered arrival times have been folded with the phase-connected timing solution given in Gotthelf et al. (2002) using only the first three frequency coefficients to obtain pulse phase distributions for selected energy windows. Combining now the phase distributions from the various PCUs, the well-known 2–10 keV profile of 1E 1841−045 (see Gotthelf et al. 2002) could be recognized in each subobservation; however, phase shifts between the subobservations made a direct combination impossible. Therefore we correlated the pulse phase distribution of each subobservation with a chosen initial template and applied the measured phase shifts to obtain an aligned combination with much higher statistics. The correlation is then repeated once with, instead of the initially chosen template, the aligned combination from the first correlation to obtain the final summed profile (see, e.g., de Plaa et al. 2003 for a similar iterative method applied for PSR B0540−69). The summed profile for energies between 3.9 and 7.8 keV deviates from uniformity at a $\sim 32\ \sigma$ level and is shown in Figure 1. Its morphology mimics the profile shown by Gotthelf et al. (2002). For the first time, however, pulsed emission has been detected up to $\sim$25 keV—the deviation from uniformity is 9.5 and 3.2 σ in the 11.7–16.1 and 16.1–23.8 keV energy ranges, respectively—providing strong evidence for a nonthermal origin of the pulsed high-energy emission. This result motivated us to search also the higher energy HEXTE data for a pulsar signal.

3.2. *Timing Analysis of HEXTE Data*

HEXTE operated in its default rocking mode during the observations listed in Table 1, allowing the collection of

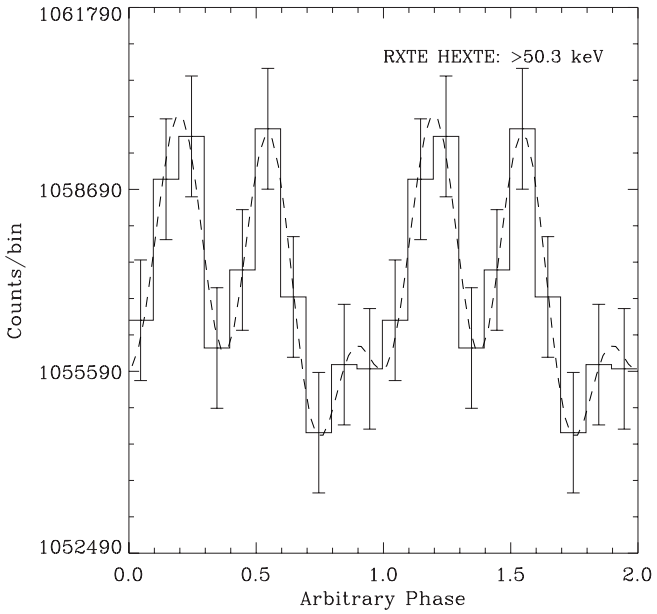

FIG. 2.—*RXTE* HEXTE pulse profile of 1E 1841−045 for energies greater than 50.3 keV demonstrating the existence of pulsed emission from this source at hard X-rays/soft gamma-rays. The deviation from uniformity is about 4.1 σ. The dashed line represents the best-fitting truncated Fourier series (three harmonics), like that shown in Fig. 1. The structured profile and the minimum level approximately coincide in phase with those in the 3.9–7.8 keV profile of Fig. 1.

real-time background data from two independent positions $\pm 1\overset{\circ}{.}5$ to either side of the on-source position. For the timing analysis we selected only the on-source data. Good time intervals have been determined using screening filters similar to those used in the case of the PCA. The selected on-source HEXTE event times have subsequently been barycentered and folded according to the ephemeris given in Gotthelf et al. (2002), again using only the first three frequency coefficients. Applying the phase shifts as derived from the contemporaneous PCA measurements to the HEXTE phase distributions of each subobservation, we could obtain the HEXTE pulse phase distributions in 256 spectral channels for the combination of observations listed in Table 1. The HEXTE integral ($\gtrsim$15 keV) pulse profile deviates from uniformity at a $\sim$4.7 σ level and shows strong similarities with the PCA profile for energies above $\sim$10 keV. Most remarkably, the pulse profile for energies greater than 50.3 keV reaches a significance of $\sim$4.1 σ, proving the existence of pulsed emission from 1E 1841−045 at hard X-rays/soft gamma-rays (see Fig. 2).

3.3. *Energy Dependence of the Pulse Profile Morphology*

We have investigated the morphology of the pulse phase distributions as a function of energy using both the *RXTE* PCA and HEXTE data. This kind of information could provide clues to the origin and physics of the processes responsible for the pulsed high-energy radiation. In Figure 3 a collage of pulse-phase distributions is shown for different energy bands between $\sim$2 and $\sim$250 keV.[4] A striking feature is that pulse minimum occurs in the phase range [0.7, 0.8] irrespective of the energy band. Furthermore, the structured broad profile, measured with high statistics in the PCA data, seems to behave as two components ("pulses") separated $\sim$0.4 in phase, with the relative contributions varying with energy. The first "pulse" near phase 0.1 is dominant over the second "pulse" near phase 0.5 for energies below $\sim$9 keV. Above this energy the second pulse, however, has an intensity level similar to that of the first pulse. Quantitatively this behavior is shown in Figure 4, where the

[4] For HEXTE the 26–35.2 energy window is ignored in this collage because of a huge background line near 30 keV due to the activation of iodine.

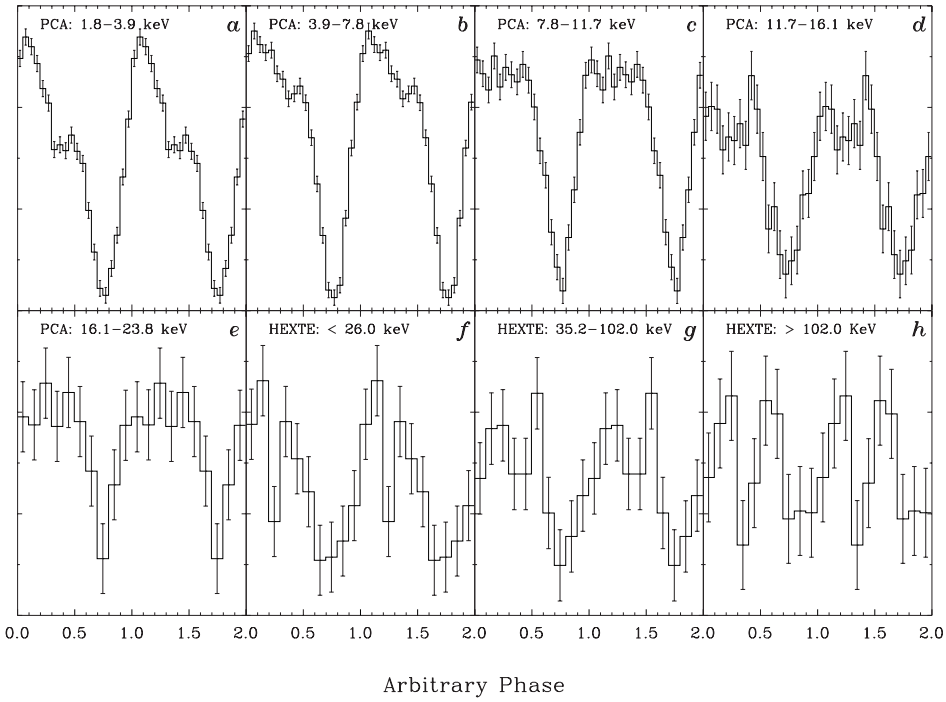

FIG. 3.—*RXTE* PCA/HEXTE collage of pulse profiles of 1E 1841−045 for energies greater than 1.8 keV. Two cycles are shown for each panel. (*a*–*e*) *RXTE* PCA pulse profiles for energies between 1.8 and 23.8 keV. (*f*–*h*) *RXTE* HEXTE pulse profiles for the energy ranges less than 26, 35.2–102, and greater than 102 keV. The three HEXTE profiles deviate from uniformity at the 4.2, 3.1, and 2.7 σ levels, respectively. Note the morphology change of the pulse profiles, particularly in the PCA profiles.

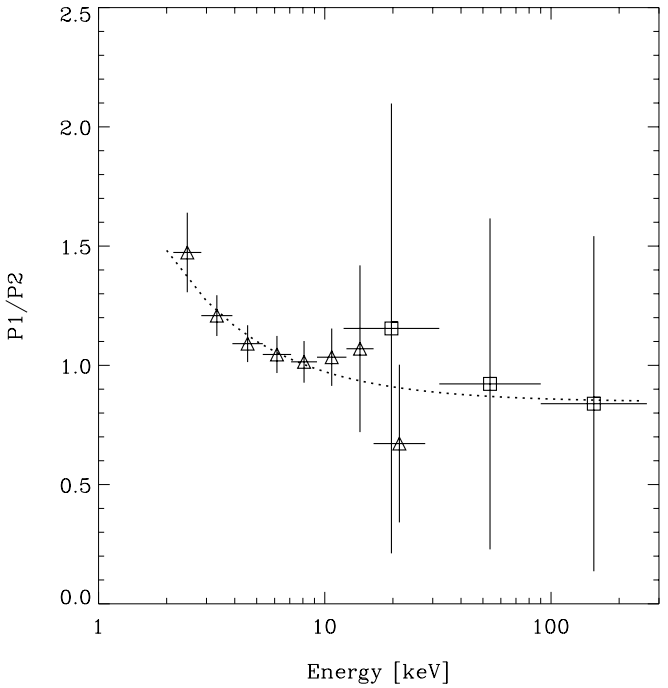

FIG. 4.—Ratio of excess counts in phase range 0.8–1.25 (P1) and 0.25–0.7 (P2) for *RXTE* PCA (*triangles*) and HEXTE (*squares*) data as a function of energy. The dotted line represents the best fit to a function of the form $a + b/E$ with (a, b) parameters to be optimized. The improvement relative to a constant function a is about 3 σ.

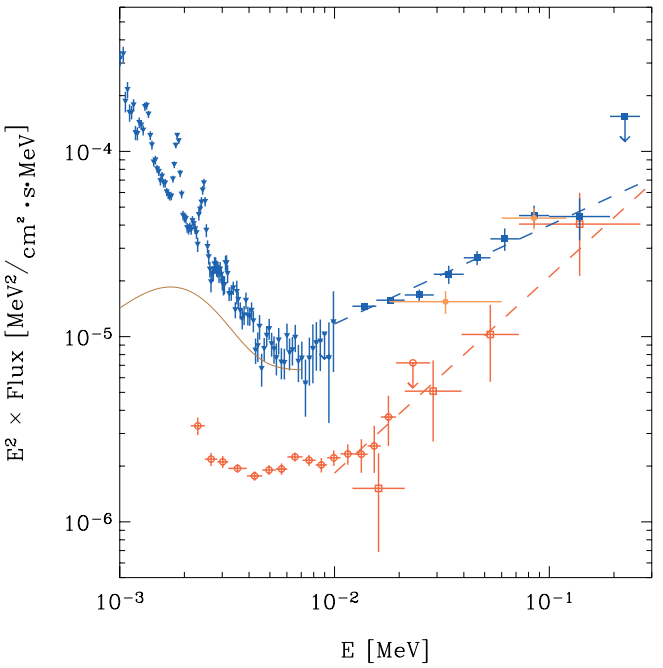

FIG. 5.—A νF_ν spectral representation of the total pulsed high-energy emission from 1E 1841−045 is shown in red (*RXTE* PCA, *open circles*; *RXTE* HEXTE, *open squares*). The total spectrum from the Kes 73/1E 1841−045 complex is represented in blue (*XMM* EPIC pn, *triangles*; RXTE HEXTE, *filled squares*). The total (pulsed plus DC) 1–7 keV X-ray spectrum from 1E 1841−045 (Morii et al. 2003) is plotted as a solid dark orange line. The two orange flux points are *INTEGRAL* IBIS ISGRI measurements given in Molkov et al. (2004). Fits (>10 keV) to the total complex (*blue*) and total pulsed (*red*) spectra of 1E 1841−045 are drawn as dashed lines.

ratio of the number of excess counts in phase range 0.8–1.25 (P1) and 0.25–0.7 (P2) for *RXTE* PCA and HEXTE data is plotted as a function of energy (phase range 0.7–0.8 is chosen as a DC-reference window).

The χ^2 of a fit to a function parameterized as $a + b/E$ improves by about 3 σ (1 degree of freedom) relative to the χ^2 of a fit assuming a constant, i.e., no energy dependence of the ratio. Thus, we conclude that the morphology of the high-energy (>2 keV) pulse profiles of 1E 1841−045 changes with energy.

4. SPECTRAL ANALYSIS

In this section high-energy (∼1–250 keV) spectra are presented for (1) the total pulsed emission from 1E 1841−045 based on *RXTE* PCA and HEXTE data and (2) the total high-energy emission from the Kes 73 supernova remnant plus the embedded AXP 1E 1841−045 using *RXTE* HEXTE on/off data and *XMM-Newton* pn data.

4.1. *Pulsed X-Ray Spectrum of 1E 1841−045*

The number of pulsed counts in the differential PCA/HEXTE energy bands has been determined by fitting a truncated Fourier series, $a_0 + \sum_{k=1}^{N} a_k \cos(2\pi k\phi) + b_k \sin(2\pi k\phi)$, with ϕ the pulse phase, to the measured pulse phase distributions. It turned out that three harmonics ($N = 3$) were sufficient to describe the measured distributions accurately for all energy intervals. For example, in Figures 1 and 2 the best-fit truncated Fourier series are shown as dashed lines for the PCA 3.9–7.8 keV and HEXTE > 50.3 keV pulse phase distributions, respectively.

In the case of the PCA we derived for each PCU the energy response matrix (energy redistribution including the sensitive area) for the combination of observations listed in Table 1 and subsequently took the different PCU (screened) exposure times into account in the construction of the weighted PCU-combined energy response. The pulsed excess counts per energy band are fitted in a procedure assuming an absorbed ($N_{\rm H} = 2.54 \times 10^{22}$ cm^{-2}; Morii et al. 2003) power-law photon spectrum folded through the PCU-combined energy response. The best-fit power-law model to the PCA pulsed data has a photon index of 1.93 ± 0.01. The derived 2–10 keV total pulsed flux[5] is $(5.20 \pm 0.14) \times 10^{-12}$ ergs cm^{-2}s, which is consistent with the 2–10 keV pulsed flux of $(5.70 \pm 0.70) \times 10^{-12}$ ergs cm^{-2}s given in Gotthelf et al. (2002), who used a smaller data set and a different extraction method (on/off).

In the spectral "deconvolution" process of the HEXTE total pulsed counts the on-axis[6] cluster A and B energy response matrices have been employed taking into account the (slightly) different screened on-source exposure times of each cluster. The exposure times have been corrected for the considerable dead-time effects.

The total pulsed PCA and HEXTE flux measurements are shown in Figure 5 as red open circles and squares, respectively. In this νF_ν spectral representation the hardening of the pulsed flux near 10 keV is striking. A power-law model fitted to the PCA/HEXTE total pulsed flux measurements for energies above 10 keV yielded a photon index of 0.94 ± 0.16. Such a spectral hardening has not been observed yet for any of the AXPs currently known.

[5] Spectral cross-calibration between the *BeppoSAX* MECS and *RXTE* PCA instruments indicates that the normalization of the PCA spectra is about 20% higher than that of the MECS. The PCA fluxes are therefore multiplied by 0.81 (see, e.g., Kuiper et al. 2004, about this subject).

[6] It was not necessary to derive off-source HEXTE response matrices taking into account the reduction in the sensitive area due to the collimator response because all observations were performed nearly on-axis.

4.2. *Total X-Ray Spectrum of Kes 73 plus 1E 1841−045*

For HEXTE a model-independent way for deriving the total flux from the Kes 73/1E 1841−045 complex exists based on the source on/off observations. The off-source observations make it possible to obtain instantaneous background estimates. Subtracting the properly scaled background contribution (every 32 s on-source observation is accompanied by a 28 s off-source observation; 4 s is consumed in the slew process) from the on-source measurements yielded the total excess counts from the Kes 73/1E 1841−045 complex for energies above $\gtrsim$15 keV. These excess counts have been converted to flux values using similar procedures as discussed before and the resulting flux measurements are shown as blue filled squares in Figure 5. A power-law fit through these points yielded a photon index of 1.47 ± 0.05, slightly softer than the pulsed emission for energies above 10 keV.

In order to extend the total emission spectrum toward lower energies we analyzed archival *XMM-Newton* data from an observation targeted at 1E 1841−045. We used data taken on 2002 October 5, starting at 03:16:47 UTC. We processed the data using the latest version of the *XMM-Newton* analysis software, SAS 6.0.0. For the analysis, we first produced light curves in different energy bands of a region in the sky far from the supernova remnant to check for solar flares that might have affected the observation. Since no flares were detected in the light curves, we used the total length of the observation, ∼4000 s of on-source time, for the rest of the analysis. We produced images and spectra both for the EPIC pn and the two EPIC MOS instruments, and checked that all instruments yielded consistent results. Since the EPIC pn has the largest overall effective area and is sensitive to higher energies than MOS, we concentrated only on this instrument for the rest of our analysis.

We extracted a spectrum of a circular region of 2′ radius centered on 1E 1841−045 containing both the AXP and the supernova remnant. We checked that the spectrum is not affected by pileup.[7] To produce a background spectrum we selected an area near the supernova remnant, but sufficiently far from it to avoid contamination from the supernova itself. Next we produced an energy response matrix and an ancillary response file, the latter properly weighted using the surface brightness distribution of the extended emission of the source over the detector. We rebinned the spectrum such that we had about three bins per resolution element. Since the source is relatively bright, with this rebinning we obtained at least 25 counts per bin in the range 0.3–7 keV and at least 16 counts per bin up to 11 keV. The "deconvolved" spectrum (νF_ν) is shown in Figure 5: it displays a relatively bright continuum, on top of which several emission lines of Mg, Ar, S, and Si coming from the supernova remnant can be seen.

5. DISCUSSION

We have presented the surprising discovery of very hard (photon index 0.94 ± 0.16) pulsed hard X-ray emission extending up to energies of ∼150 keV from the AXP 1E 1841−045, obtained using archival monitoring observations by the PCA and HEXTE on board *RXTE*. Such hard, nonthermal emission can only originate within the magnetosphere of a neutron star/magnetar. In fact, the total pulsed X-ray spectrum of 1E 1841−045 is very reminiscent of that of young spin-down powered pulsars. Particularly, the spectrum of the Vela pulsar with a blackbody spectrum at lower X-ray energies and a hard power-law extension to higher energies looks very similar. These hard power-law spectral extensions with photon indices of ∼1 are also found for the young (radio-weak/quiet) spin-down powered pulsars PSR B1509−58 (Kuiper et al. 1999), PSR B1846−0258, PSR J1811−1925, and PSR J1930+1852 (Kuiper & Hermsen 2004), all associated with SNRs, like 1E 1841−045, and the old millisecond pulsars PSR J0218+4232, PSR B1821−24, and PSR B1937+21 (Kuiper et al. 2004).

Such hard X-ray emission from AXPs has hardly been considered in the modeling of AXPs. However, Cheng & Zhang (2001) studied the production of high-energy gamma-ray radiation in the outer magnetospheres of AXPs. They argue that because of the strong field of a magnetar, the gamma-ray emission rooted at the polar caps will be quenched. However, far away from the pulsar surface, i.e., in the outer gaps, the gamma-rays could be emitted because the local magnetic field will drop below the critical quantum limit. The production process would be curvature radiation by the acceleration of electrons/positrons, resulting from the collisions between high-energy photons from the outer gap and the soft X-rays originating from the stellar surface. They applied their model calculations also to the case of 1E 1841−045, and predict an integral gamma-ray photon flux for energies above 100 MeV of $\sim 8.7 \times 10^{-9}$ $(d/6\ \mathrm{kpc})^{-2}$ cm^{-2} s^{-1}, which is below the EGRET sensitivity but above the sensitivity of *GLAST*. The very hard pulsed spectrum we measured with HEXTE might be consistent with this interpretation.

We studied the energy dependence of the pulse profile morphology and confirm the findings by Morii et al. (2003), namely, the pulse profile is double-peaked, and the second pulse has a harder spectrum for energies below ∼7 keV. However, this trend does not continue above ∼10 keV. Within the statistics, both pulses remain visible at about the same strengths up to ∼150 keV. Significant variations with energy of pulse profile morphologies below ∼8 keV have been reported earlier for three other AXPs, 4U 0142+61 (Israel et al. 1994, 1999), 1RXS 170849−400910 (Sugizaki et al. 1997; Israel et al. 2001), and 1E 2259.1+586 (Hanson et al. 1988), and more recently by Gavriil & Kaspi (2002) for all three sources.

The set of spectra shown in Figure 5 summarizes our present knowledge on the contributions from the different components constituting the total emission from the direction of Kes 73 and AXP 1E 1841−045, i.e., the pulsed and DC components of 1E 1841−045, and the emission from SNR Kes 73. In addition to the total pulsed spectrum (PCA/HEXTE) and the pulsed+DC+Kes-73 spectrum (XMM EPIC pn/HEXTE) derived in this work, we show the *INTEGRAL* IBIS ISGRI flux values for energies 18–120 keV (Molkov et al. 2004) and the *Chandra* ACIS spectrum (Morii et al. 2003) for the pulsed+DC spectrum of 1E 1841−045. We note that the *INTEGRAL* flux points are consistent with our total HEXTE spectrum (one should realize that these preliminary *INTEGRAL* IBIS ISGRI flux values have still systematic uncertainties of ∼10%).

For energies up to about 7 keV we have information on the relative contributions: (1) the pulsed fraction of 1E 1841−045 is ∼25%, and (2) there is very little margin for emission from SNR Kes 73 around 7 keV. This suggests that the HEXTE spectrum above 15 keV is dominated by emission from 1E 1841−045 (pulsed+DC), and above ∼100 keV the spectrum is totally due to pulsed emission. This would also mean that the

[7] Pileup occurs when two or more photons hit the same CCD pixel within a read-out cycle. In that case the instruments count those photons as single event with an energy approximately equal to the sum of the energies of the individual photons. Pileup reduces the apparent flux of the source and at the same time makes the spectrum appear harder than it really is.

DC emission from 1E 1841−045 extends up to ∼100 keV! An alternative interpretation is that the relative contribution from Kes 73 increases again above 10 keV because of a new hard component. Although the latter seems unlikely, higher spatial resolution measurements at energies above 10 keV are required to exclude this possibility.

If we assume that the contribution from Kes 73 is small or negligible above 10 keV, the challenge is now to explain the hard DC emission from 1E 1841−045. Most plausible might be an origin in the magnetosphere, namely, for the situation that the pulsed emission is "on" for all phases. In the competing polar cap (e.g., as discussed for AXPs by Zhang & Harding 2000) and outer gap (see, e.g., Cheng & Zhang 2001) scenarios explaining the high-energy emission from spin-down powered pulsars, there are geometries for which this is indeed possible. Allowing for a small contribution from Kes 73, e.g., up to about 30 keV, and knowing that pulsar spectra depend on pulse phase, detailed model calculations are required to investigate this interpretation further.

This research has made use of data obtained from the High Energy Astrophysics Science Archive Research Center (HEASARC), provided by NASA's Goddard Space Flight Center.

REFERENCES

Cheng, K. S., & Zhang, L. 2001, ApJ, 562, 918
Gavriil, F. P., & Kaspi, V. M. 2002, ApJ, 567, 1067
Gavriil, F. P., Kaspi, V. M., & Woods, P. M. 2002, Nature, 419, 142
———. 2004, Adv. Space Res., 33, 654
Gotthelf, E. V., et al. 2002, ApJ, 564, L31
Hanson, C. G., Dennerl, K., & Coe, M. J. 1988, A&A, 195, 114
Israel, G. L., Mereghetti, S., & Stella, L. 1994, ApJ, 433, L25
Israel, G. L., Oosterbroek, T., & Angelini, L. 1999, A&A, 346, 929
Israel, G. L., et al. 2001, ApJ, 560, L65
Jahoda, K., et al. 1996, Proc. SPIE, 2808, 59
Kaspi V. M., et al. 2003, ApJ, 588, L93
Kuiper, L., & Hermsen, W. 2004, A&A, submitted
Kuiper, L., Hermsen, W., & Stappers, B. 2004, Adv. Space Res., 33, 507
Kuiper, L., et al. 1999, A&A, 351, 119
Kulkarni, S. R., et al. 2003, ApJ, 585, 948
Mereghetti, S., et al. 2002, Proc. 270 WE-Heraeus Seminar on Neutron Stars, Pulsars, and Supernova Remnants, ed. W. Becker, H. Lesch, & J. Trümper (Garching: MPI), 29
Molkov, S. V., et al. 2004, preprint (astro-ph/0402416)
Morii, M., et al. 2003, PASJ, 55, L45
de Plaa, J., Kuiper, L., & Hermsen, W. 2003, A&A, 400, 1013
Rothschild, R. E., et al. 1998, ApJ, 496, 538
Sanbonmatsu, K. Y., & Helfand, D. J. 1992, AJ, 104, 2189
Sugizaki, M., et al. 1997, PASJ, 49, L25
Thompson, C., & Duncan R. C. 1996, ApJ, 473, 322
Vasisht, G., & Gotthelf, E. V. 1997, ApJ, 486, L129
Woods, P. M. 2004, Adv. Space Res., 33, 630
Zhang, B., & Harding A. K. 2000, ApJ, 535, L51

Note added in proof.—After submission of this paper we detected similarly hard pulsed X-ray emission from two other AXPs, namely, 1RXS J170849−400910 and 4U 0142+61 (L. Kuiper et al. 2004, in preparation).